Electronic Supplementary Information (ESI)

Multifunctional ultrasmall-MoS_2/graphene composites for high sulfur loading Li-S batteries

Tianyu Tang,[a] Teng Zhang,[a] Lina Zhao,[a] Biao Zhang,[a] Wei Li,[a] Junjie Xu,[a] Long Zhang,[a] Hailong Qiu,[b] Yanglong Hou*[a]

a. *Beijing Key Laboratory for Magnetoelectric Materials and Devices (BKLMMD), Beijing Innovation Center for Engineering Science and Advanced Technology (BIC-ESAT), Department of Materials Science and Engineering, College of Engineering, Peking University, Beijing 100871, China. E-mail: hou@pku.edu.cn.*

b. *Clean Nano Energy Center, State Key Laboratory of Metastable Materials Science and Technology, College of Materials Science and Engineering, Yanshan University, Qinhuangdao 066004, China.*

Supplementary Figure

Experimental Section

Preparation of NGM: The graphene oxide (GO) was prepared by the modified Hummer's method [1]. Then the 100 mg GO was mixed with 1.5 g dicyandiamide in 60 mL deionized water followed with sonication of 30 minutes. The 1.5 g Pluronic F127 (PF127, PEO−PPO−PEO) was mixed with 5 mL ethanol followed with sonication of 30 minutes when the solution was clear. After mixing two types of solutions prepared before, the mixture was sealed in 100 mL Teflon-lined autoclave heated at 180 ℃ for 18 h. After the hydrothermal process, the resulted product was freeze drying. Finally, the dry sample was annealed at 800 ℃ for 2 h under the atmosphere of NH_3.

Preparation of MoS_2-G: The 100 mg GO was dispersed in 80 mL deionized water followed with sonication for 30 minutes. The 1.5 g Pluronic F127 (PF127, PEO−PPO−PEO) was mixed with 5 mL ethanol followed with sonication of 30 minutes when the solution was clear. After mixing two types of solutions, it was added with the hexaammonium molybdate of 100 mg and the 20 mL of N,N,N-trimethyl-1-dodecanaminium bromide with the concentration of 37.5 g L^{-1} was poured into the mixture. After vigorous stirring for 12 hours, the product was collected by centrifuged and washed by deionized water for three times. Then the sediment was freeze drying. The dry sample was annealed at 800 ℃ for 2 h under the atmosphere of N_2. After the synthesis process, the resulted products were sulfurized at 600 ℃ for 2 h under the atmosphere of N_2 with the crucible containing sulfur powders in front of it.

Polysulfide adsorption test: The Li_2S and sulfur with a molar ratio of 1:5 was dissolved in 1,2-dimethoxyethane under stirring at 40 ℃ for 3 days to prepare Li_2S_6 solution. Then the as-prepared Li_2S_6 solution was diluted to 1 mmol L^{-1}. The NGM and Mo-G were added into the two bottles of Li_2S_6 solution and let them statically.

Materials Characterization: The scanning electron microscope (SEM) images and the transmission electron microscope images (TEM) were delivered by a field-emission scanning electron microscope (Merlin Compact, ZEISS) and FEI Tecnai T20 at 200 kV, respectively. The X-ray diffraction was utilized to analyze the phase of prepared product by Rigaku DMAX-2400 X-ray diffractometer equipped with Cu Kα (λ = 1.5405 Å) radiation. The X-ray photoelectron spectroscopy (XPS) measurements were performed to analyze the surface chemistry with monochromatized Al Kα radiation (Axis Ultra DLD, Kratos Analytical Ltd.). The surface area was analyzed by the Brunauer–Emmett–Teller (BET) measurement. Raman spectroscopy was performed on a

LabSpec6 (Horiba) with a 560 nm laser. The sulfur content was determined by thermogravimetric analysis (TGA) using a Q600 Simultaneous DSC-TGA under N_2 flow. The UV-2550 was utilized to characterize the ultraviolet/visible absorption spectra of Li_2S_6 solution before and after adding NGM and MoS_2-G.

Electrochemical Characterization: The NGM-sulfur composite which was prepared at 155 ℃ for 12 h was mixed with MoS_2-G with a mass ratio of 10:1 and stirred in N-methyl-2-pyrrolidone for 6 hours to prepare MoS_2-G/NGM-S. Then the working electrode slurry was prepared by mixing the MoS_2-G/NGM-S (or NGM-S, or MoS_2-G-S), conductive agent (ketjen black), and PVDF with the mass ratio of 7.5:1.5:1, which were pasted on carbon cloth and dried in vacuum oven at 60 ℃ for 12 h. The sulfur loading of each electrode was at 1.2-1.6 mg cm^{-2}. By utilization of lithium metal as a counter electrode, the CR-2032 coin cells with the electrolyte contained 1M lithium bis(trifluoromethanesulfonyl)imide (LITFSI) and 2 wt% $LiNO_3$ in the solution of dimethoxyethane and 1,3-dioxolane with the volume ratio of 1:1 was assembled in an argon filled glovebox. The electrolyte/sulfur ratio of the cathode with low mass loading is 20 µL mg^{-1} and the electrolyte/sulfur ratio of the MoS_2-G/NGM-S-5 is increased to 25 µL mg^{-1}. The cyclic voltammetry (CV) measurements were carried out with a scan rate of 0.1 mV s^{-1} between 1.8-2.8 V vs. Li^+/Li on a Bio-logic VSP multichannel potentionstatic-galvanostatic system. The cycling performance and rate capability were performed between 1.8-2.8 V vs. Li^+/Li by LAND CT 2001A.

Assemblying of symmetrical cell: Each material including MoS_2-G, NGM and rGO was utilized as electrodes in the symmetrical cells without sulfur. The weight ratio of each material and the PVDF binder was 3:1. Both working electrode and counter electrode were identical materials. In the meanwhile, the electrolyte contained 0.5 mol L^{-1} Li_2S_6, 1M lithium bis(trifluoromethanesulfonyl)imide (LITFSI) and 2 wt% $LiNO_3$ in the solution of dimethoxyethane and 1,3-dioxolane with the volume ratio of 1:1. The cyclic voltammetry (CV) measurements of symmetrical cells were carried out with a scan rate of 50 mV s^{-1} between -0.7-0.7 V. The EIS tests were delivered by a Bio-logic VSP multichannel potentionstatic-galvanostatic system with the frequency range of 1 mHz to 1MHz with the amplitude of 5 mV.

Theoretical calculations: The density functional theory (DFT) calculations were performed to calculate the adsorption binding energy between sulfur host materials (N-doped graphene and MoS_2) and Li_2S_6 implemented in the Vienna ab initio Simulation Package (VASP) [2, 3]. The Perdew-Burke-Ernzerhof functional was used to describe the exchange correlation energy and the cutoff energy of the plane wave basis was set as 400 eV [4]. The k-point mesh 1 x 2 x 1 was delivered for nitrogen-doped graphene and MoS_2. The adsorption binding energy was defined as $E_{ads} = E_{total} - E_{host} - E_{LIP}$, where E_{total} represents the total energy of the adsorbed composites which consist of host materials and Li_2S_6, E_{host} represents the energy of the isolated host materials and E_{LIP} represents the energy of the isolated Li_2S_6.

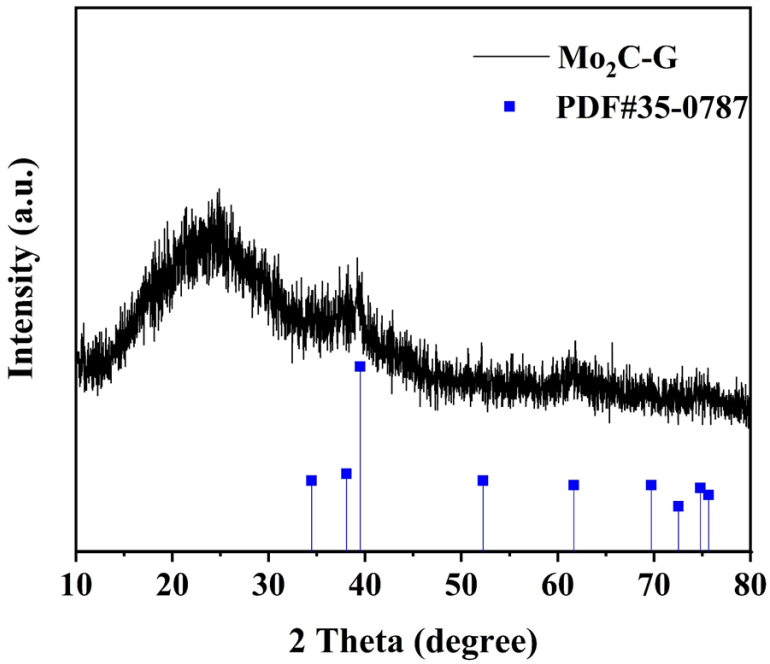

Fig. S1. XRD pattern of Mo_2C-G.

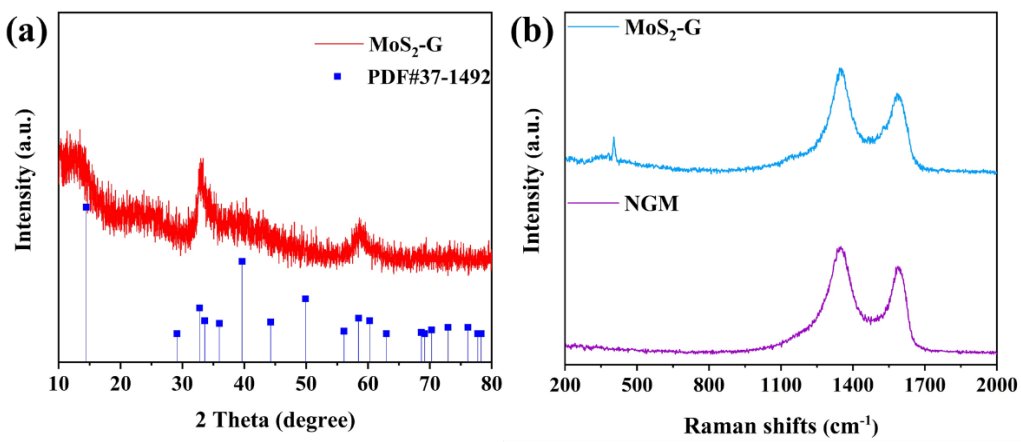

Fig. S2. (a) XRD pattern of MoS_2-G. (b) Raman spectra of MoS_2-G and NGM.

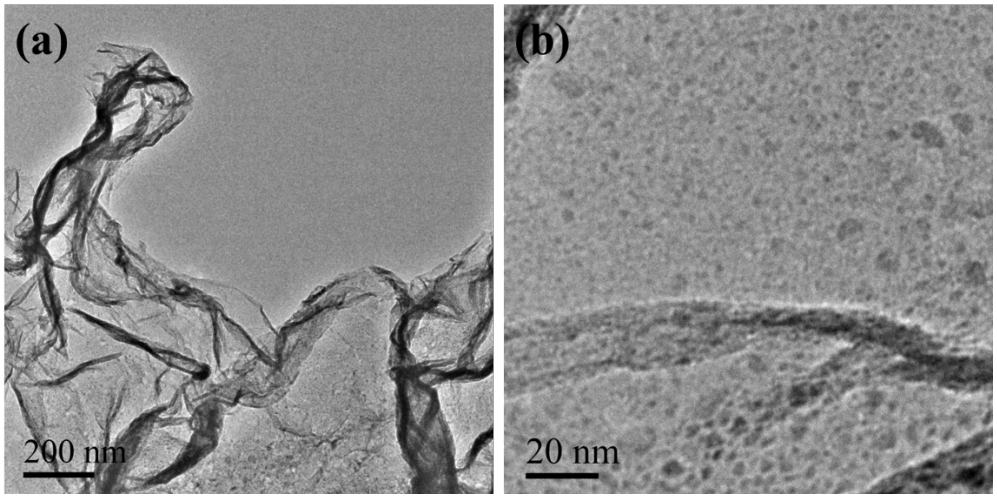

Fig. S3. TEM images of Mo_2C-G.

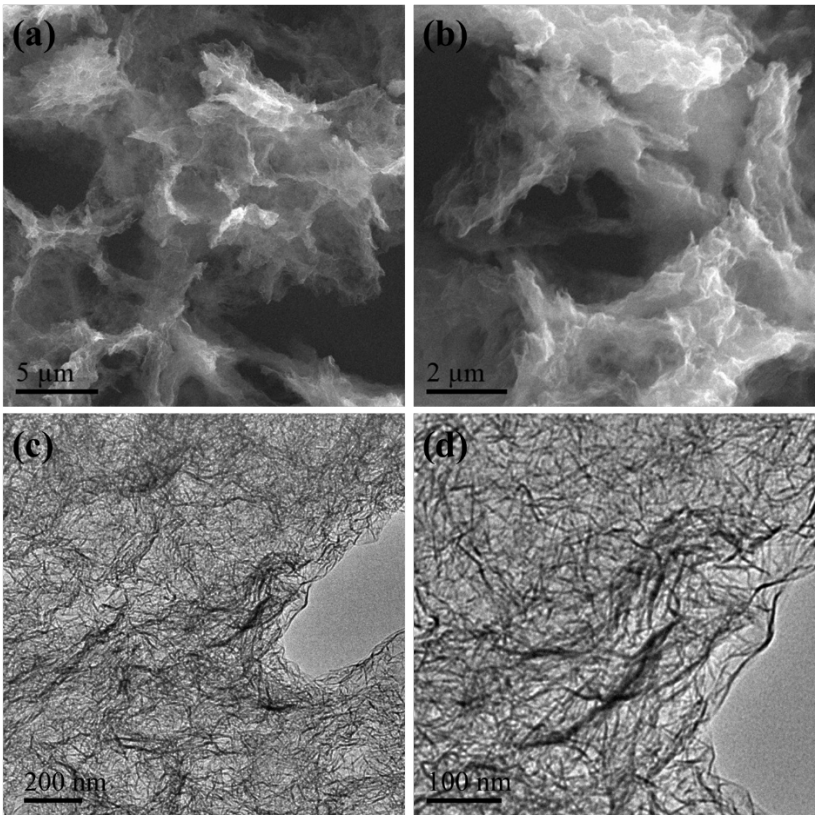

Fig.S4. (a-b) SEM images of NGM. (c-d) TEM images of NGM.

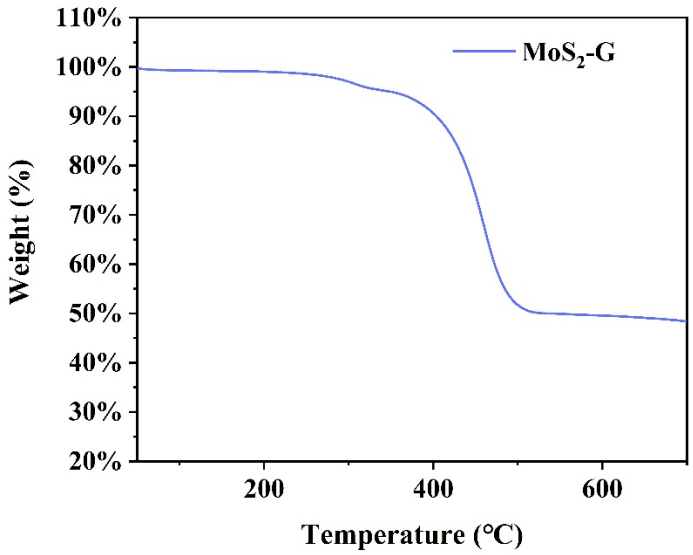

Fig. S5. The TGA curve of MoS_2-G obtained under air flow.

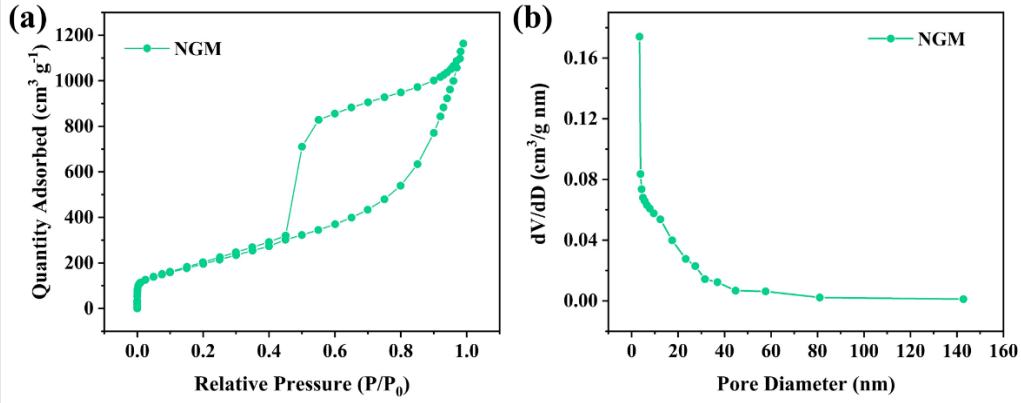

Fig. S6. (a) Nitrogen adsorption−desorption isotherms, and (b) pore size distribution of the NGM.

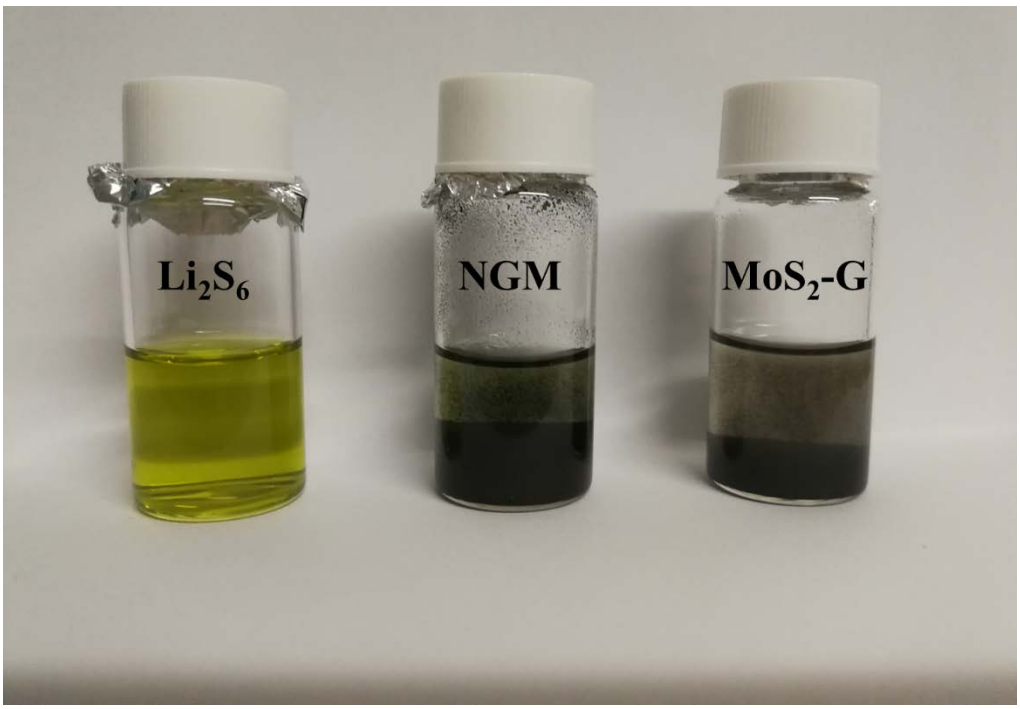

Fig. S7. The photograph of Li_2S_6 solution before and after adding NGM and MoS_2-G.

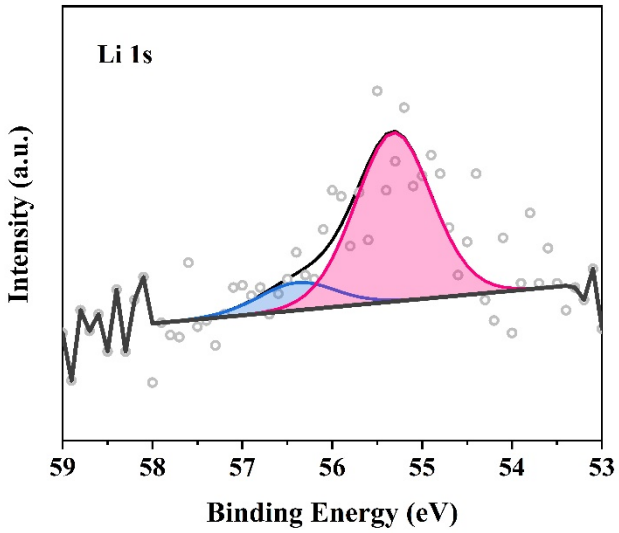

Fig. S8. The high resolution of Li 1s spectrum of the NGM/Li_2S_6.

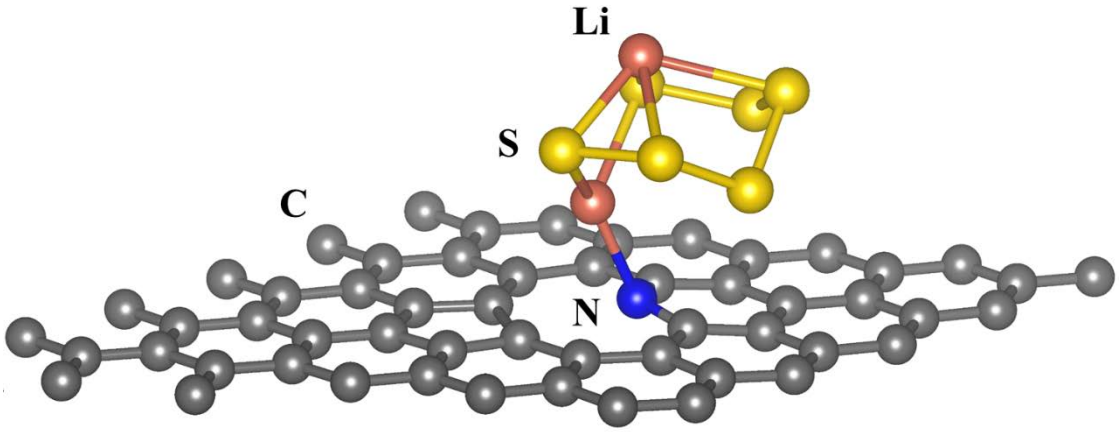

Fig. S9. The Li_2S_6 on the N-doped graphene and the interaction between Li_2S_6 and pyridinic N.

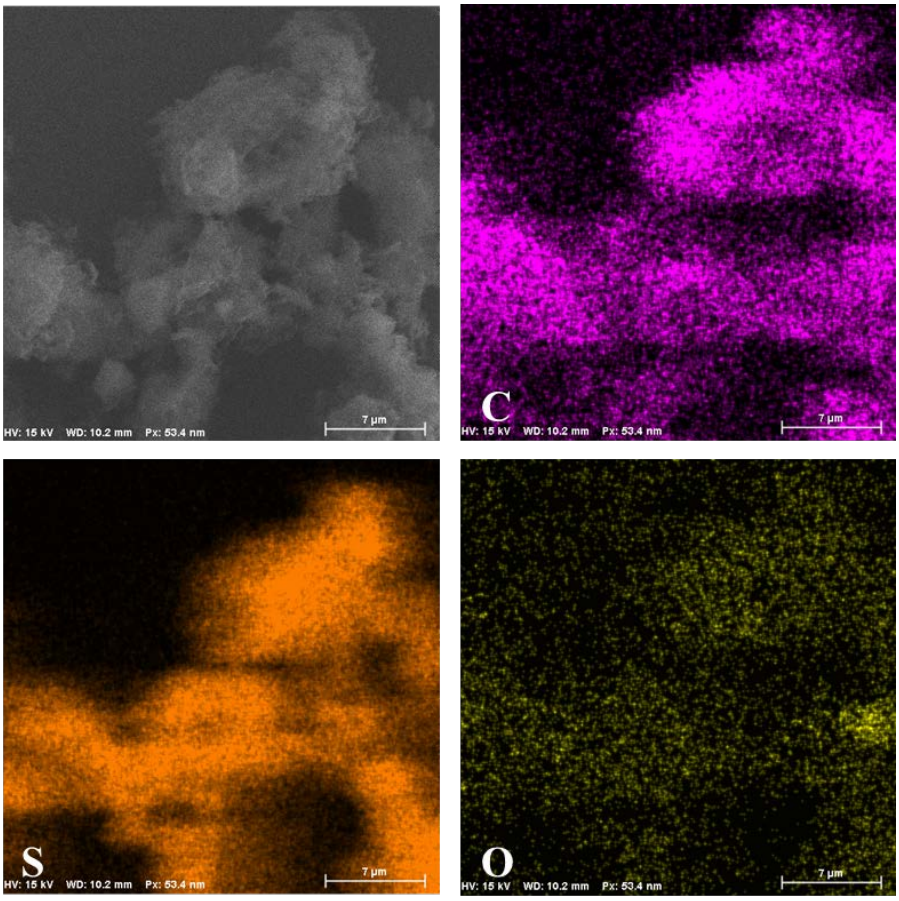

Fig. S10. The elemental mapping of the NGM-S.

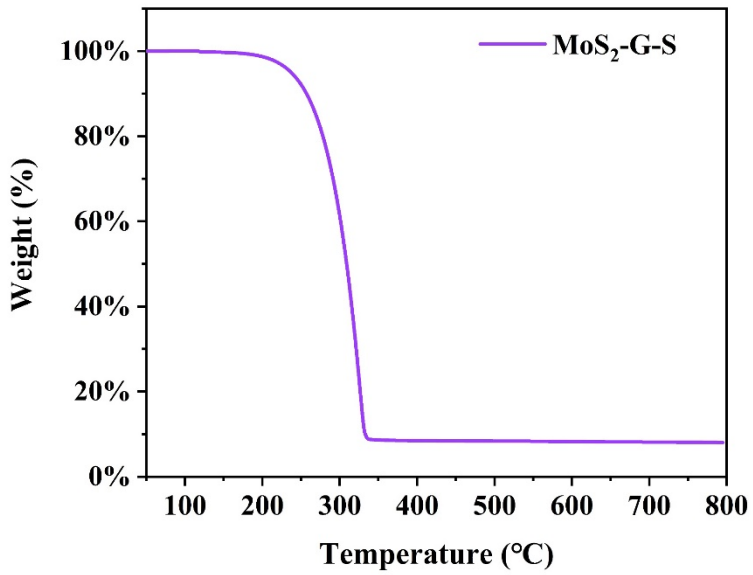

Fig. S11. The TGA curve of MoS_2-G-S obtained under N_2 flow.

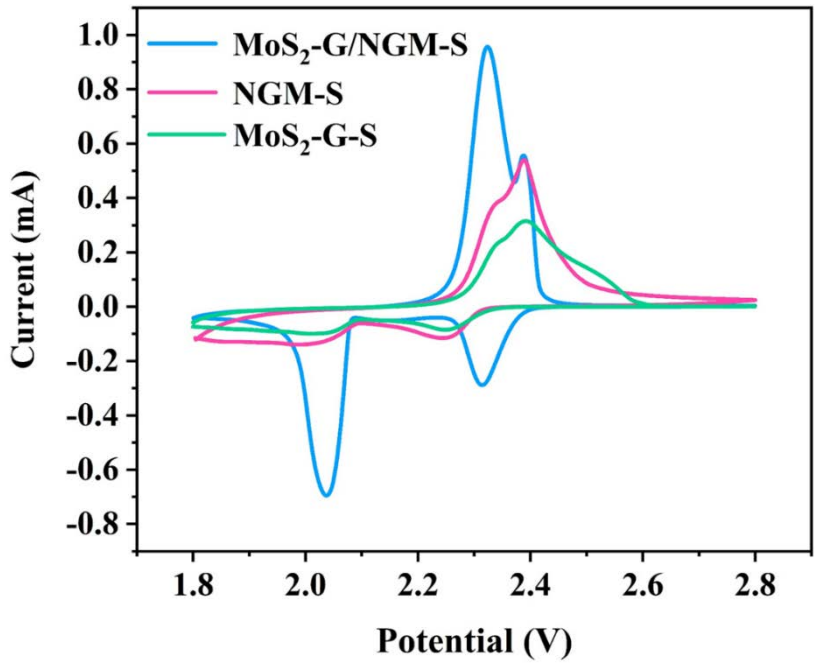

Fig. S12. The CV profiles of MoS_2-G/NGM-S, MoS_2-G-S and NGM-S cathode with a range of 1.8-2.8 V at a scan rate of 0.1 mV s^{-1}.

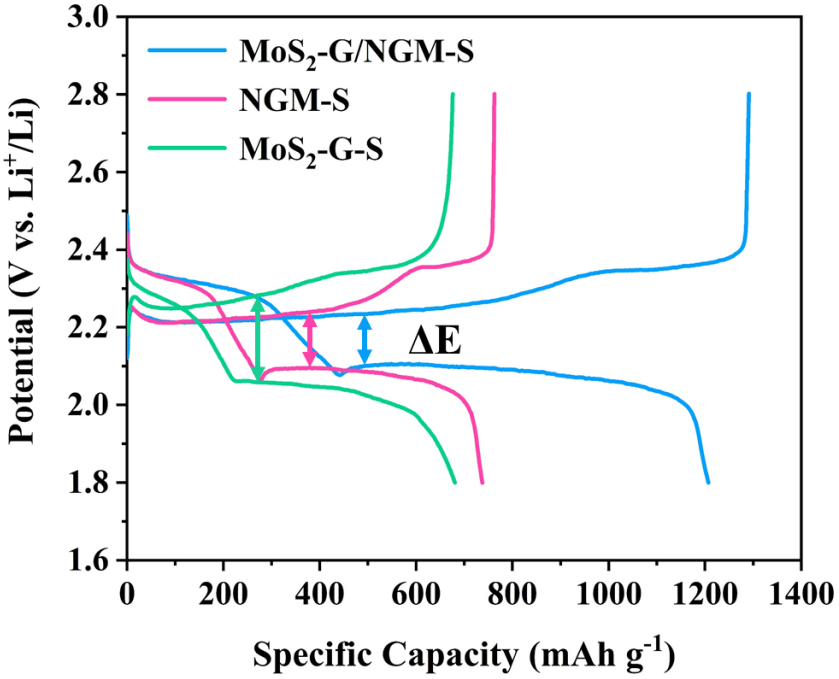

Fig. S13. The galvanostatic charge–discharge voltage profiles of MoS_2-G-S, NGM-S, and MoS_2-G/NGM-S at 0.3 C after 3 cycles.

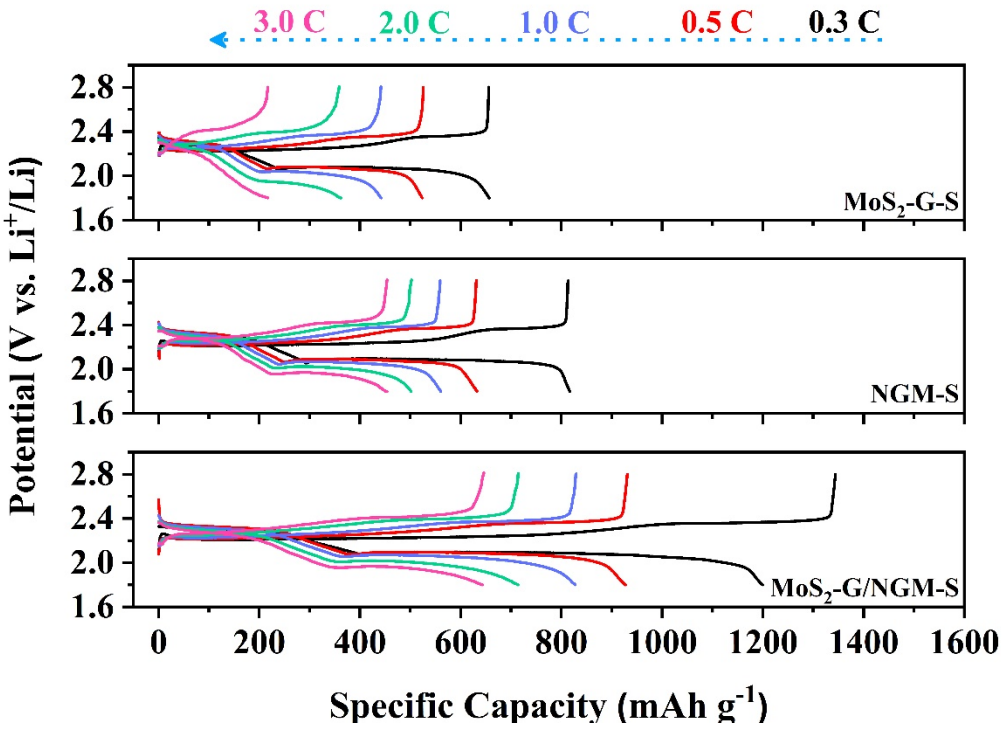

Fig. S14. The galvanostatic charge–discharge voltage profiles of MoS_2-G-S, NGM-S, and MoS_2-G/NGM-S at rates ranging from 0.3 C to 3.0 C.

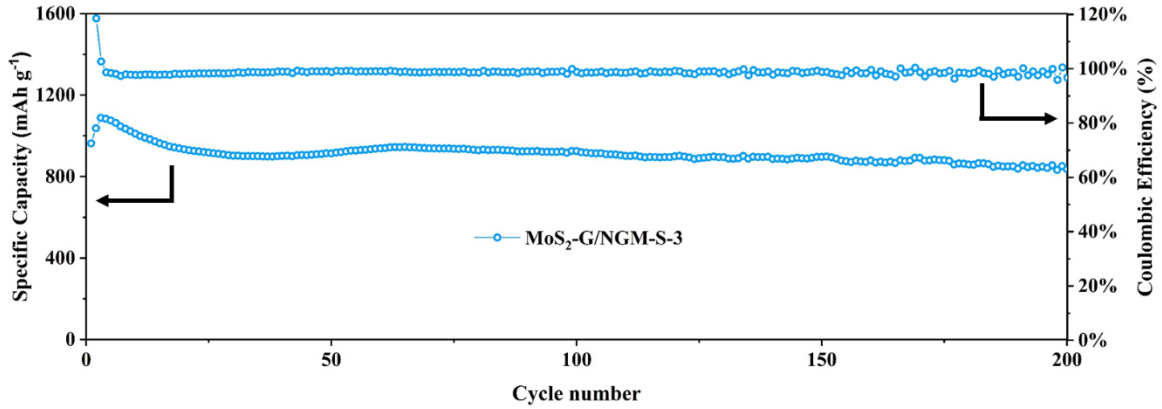

Fig. S15. The cycling performance of the MoS_2-G/NGM-S-3 at 0.3 C.

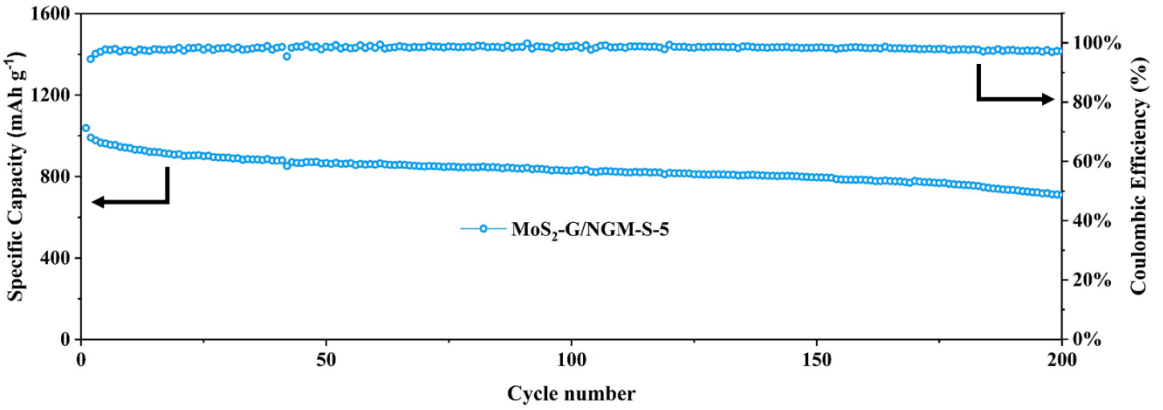

Fig. S16. The cycling performance of the MoS_2-G/NGM-S-5 at 0.3 C.

Table S1. Comparison of cathode performance with several reported works.

Cathode material	Sulfur loading content (wt%)	Total sulfur loading content in the cathode (wt%)	Area sulfur loading mass (mg cm^{-2})	Initial capacity (mAh g^{-1}/C)	Decay rate (%per cycle)	Reference
C@TiN-S	71	50	1.1	1309/0.2	0.39	5
S@C-Co/TiO_2	66	46	1.5	1209/0.5	0.44	6
$ZnCo_2O_4$@N-RGO	71	50	1.1~1.3	905/1.6 A g^{-1}	0.18	7
Co_3O_4/S/ACNT	59	47	1.5	748.7/0.5	0.064	8
PANI coating EDA-CNTs	72	58	2	992/0.5	0.15	9
VO_2 HSs@S	71	50	-	930/0.1	0.15	10
PHCN/rGO/S	72	58	3.1	900.1/0.2	0.286	11
MoS_2/S/rGO	70	56	0.9~1	1305/0.2	0.209	12
CoP@HPCN-MWCNT	70	56	2.2	887/0.2	0.076	13
MoS_2-G-S	91	68	1.2~1.6	634.9/0.3	1.20	This work
NGM-S	92	69	1.2~1.6	805.8/0.3	0.432	This work
MoS_2-G/NGM-S	92	63	3	963.5/0.3	0.070	This work

References

1. H. Yin, C. Zhang, F. Liu and Y. Hou, Hybrid of Iron Nitride and Nitrogen-Doped Graphene Aerogel as Synergistic Catalyst for Oxygen Reduction Reaction, *Adv. Funct. Mater.*, 2014, **24**, 2930-2937.
2. Y. Song, W. Zhao, L. Kong, L. Zhang, X. Zhu, Y. Shao, F. Ding, Q. Zhang, J. Sun and Z. Liu, Synchronous immobilization and conversion of polysulfides on a VO_2-VN binary host targeting high sulfur load Li-S batteries, *Energy Environ. Sci.*, 2018, **11**, 2620-2630.
3. G. Kresse and J. Furthmuller, Efficiency of ab-initio total energy calculations for metals and semiconductors using a plane-wave basis set, *Computational Materials Science*, 1996, **6**, 15-50.
4. J. P. Perdew, K. Burke and M. Ernzerhof, Generalized gradient approximation made simple (vol 77, pg 3865, 1996), *Phys. Rev. Lett.*, 1997, **78**, 1396-1396.

5. Y. Wang, R. Zhang, Y.-c. Pang, X. Chen, J. Lang, J. Xu, C. Xiao, H. Li, K. Xi and S. Ding, Carbon@titanium nitride dual shell nanospheres as multi-functional hosts for lithium sulfur batteries, *Energy Storage Materials*, 2019, **16**, 228-235.
6. R. Liu, Z. Liu, W. Liu, Y. Liu, X. Lin, Y. Li, P. Li, Z. Huang, X. Feng, L. Yu, D. Wang, Y. Ma and W. Huang, TiO_2 and Co Nanoparticle-Decorated Carbon Polyhedra as Efficient Sulfur Host for High-Performance Lithium-Sulfur Batteries, *Small*, 2019, **15**, 1804533.
7. Q. Sun, B. Xi, J.-Y. Li, H. Mao, X. Ma, J. Liang, J. Feng and S. Xiong, Nitrogen-Doped Graphene-Supported Mixed Transition-Metal Oxide Porous Particles to Confine Polysulfides for Lithium-Sulfur Batteries, *Adv. Energy Mater.*, 2018, **8**, 1800595.
8. R. Liu, F. Guo, X. Zhang, J. Yang, M. Li, W. Miaomiao, H. Liu, M. Feng and L. Zhang, Novel "Bird-Nest" Structured Co_3O_4/Acidified Multiwall Carbon Nanotube (ACNT) Hosting Materials for Lithium–Sulfur Batteries, *ACS Applied Energy Materials*, 2019, **2**, 1348-1356.
9. M. Yan, H. Chen, Y. Yu, H. Zhao, C. Li, Z. Hu, P. Wu, L. Chen, H. Wang, D. Peng, H. Gao, T. Hasan, Y. Li and B. Su, 3D Ferroconcrete-Like Aminated Carbon Nanotubes Network Anchoring Sulfur for Advanced Lithium-Sulfur Battery, *Adv. Energy Mater.*, 2018, **8**, 1801066.
10. L. Zhou, L. Yao, S. Li, J. Zai, S. Li, Q. He, K. He, X. Li, D. Wang and X. Qian, The combination of intercalation and conversion reactions to improve the volumetric capacity of the cathode in Li–S batteries, *J. Mater. Chem. A*, 2019, **7**, 3618-3623.
11. X. Bai, C. Wang, C. Dong, C. Li, Y. Zhai, W. Si and L. Xu, Porous honeycomb-like C_3N_4/rGO composite as host for high performance Li-S batteries, *Science China Materials*, 2019, **62**, 1265-1274.
12. Y. Wei, Z. Kong, Y. Pan, Y. Cao, D. Long, J. Wang, W. Qiao and L. Ling, Sulfur film sandwiched between few-layered MoS_2 electrocatalysts and conductive reduced graphene oxide as a robust cathode for advanced lithium-sulfur batteries, *J. Mater. Chem. A*, 2018, **6**, 5899-5909.
13. Z. Ye, Y. Jiang, J. Qian, W. Li, T. Feng, L. Li, F. Wu and R. Chen, Exceptional adsorption and catalysis effects of hollow polyhedra/carbon nanotube confined CoP nanoparticles superstructures for enhanced lithium-sulfur batteries, *Nano Energy*, 2019, **64**, 103965.